



# Evaluation of IMERG data in Bangladesh and surrounding regions and their application to studying diurnal variation of precipitation

Tanvir Ahmed<sup>1,2</sup> · Seong-Ho Hong<sup>1</sup> · Han-Gyul Jin<sup>1</sup> · Joohyun Lee<sup>1</sup> · Jong-Jin Baik<sup>1</sup>

Received: 14 May 2021 / Accepted: 29 July 2021

© The Author(s), under exclusive licence to Springer-Verlag GmbH Austria, part of Springer Nature 2021

## Abstract

Satellite retrieval-based precipitation data with high spatial and temporal resolutions give an opportunity for precipitation research in regions with coarse networks of precipitation measuring instruments. This study evaluates the Integrated Multi-satellitE Retrievals for Global Precipitation Measurement (IMERG) data in Bangladesh and surrounding regions and then examines the diurnal variation of precipitation in these regions using the cyclostationary empirical orthogonal function (CSEOF) analysis method. The IMERG data capture the overall patterns of the diurnal variation of precipitation well, except for the overestimation of the degree of diurnal variability in the pre-monsoon season. The spatial distribution of precipitation is also captured well, except for the drastic horizontal change in precipitation within the northeastern region of Bangladesh. These encourage the use of the IMERG data for studying precipitation characteristics in Bangladesh and surrounding regions. Through the CSEOF analysis, the pre-monsoonal precipitation is characterized by the enhanced precipitation in the northern region of Bangladesh and the Meghalaya Plateau region in the late night to early morning. The monsoonal precipitation consists of two contrasting CSEOF modes. One shows enhanced precipitation in the northern region of the Bay of Bengal during 0600–1500 LST, related to the strong westerly moisture transport over the Bay of Bengal. The other shows enhanced precipitation in the southern slopes of the Meghalaya Plateau and Himalayan Foothills during 0000–0600 LST, associated with the strong southwesterly moisture transport toward these slopes that is neither blocked nor deflected by the Arakan Mountains.

## 1 Introduction

Bangladesh is located in South Asia and is the largest deltaic country in the world. Its location and geographical features make the country one of the heaviest precipitated regions in the world. Bangladesh receives 17%, 73%, and 9% of annual precipitation amount in the pre-monsoon (March to May), monsoon (June to September), and post-monsoon (October to November) seasons, respectively (Ahmed et al. 2020). There are large variations of annual precipitation amount across the country, with maximum precipitation occurring in the northeastern region and the southeastern coastal region and minimum precipitation occurring in the western region (Tarek et al. 2017; Ahmed et al. 2020). Recent studies report

a significant decreasing trend of precipitation in the western region of Bangladesh (Chowdhury et al. 2019) and frequent precipitation extremes in the northeastern region of Bangladesh (Mohsenipour et al. 2020), making Bangladesh more vulnerable to natural disasters.

The precipitation characteristics in Bangladesh and surrounding regions have been examined using rain gauge data. Using long-term daily precipitation data from 19 rain gauge stations, Ahmed and Kim (2003) showed that the average number of rainy days in the monsoon season is 60 in the western region and 100 in the northeastern region. Shahid and Khairulmaini (2009) found a gradual increase of annual precipitation amount across the country from west to east ( $7 \text{ mm km}^{-1}$ ). The monsoonal precipitation in Bangladesh exhibits a clear diurnal variation where the precipitation maximum occurs in the late night to early morning in the northern and southeastern regions (Ahmed et al. 2020). Precipitation in Bangladesh and the Meghalaya Plateau region in the monsoon season has the submonthly scale (7–25 days) intra-seasonal oscillation (ISO) (Murata et al. 2008; Fujinami et al. 2011). Satellite-based precipitation

✉ Jong-Jin Baik  
jjbaik@snu.ac.kr

<sup>1</sup> School of Earth and Environmental Sciences, Seoul National University, 08826 Seoul, South Korea

<sup>2</sup> Department of Physics, Shahjalal University of Science and Technology, Sylhet, Bangladesh

products have been also used to examine the precipitation characteristics in Bangladesh and surrounding regions. Islam and Uyeda (2007) showed that the precipitation amount averaged over the period from March to November in Bangladesh from the Tropical Rainfall Measuring Mission (TRMM) satellite precipitation product is about 97% of that obtained from the rain gauge observation. Using the TRMM data for 13 years (1998–2010), Tarek et al. (2017) showed that the TRMM data reproduce the spatial and temporal distributions of precipitation and are reliable for use in hydrological analyses of watersheds in Bangladesh.

Reliable precipitation data are a precondition for precipitation studies in and around Bangladesh. Rain gauge data have been considered to be most consistent and precise (He et al. 2011). However, the sparse distribution of rain gauge stations provides incomplete spatial variations of precipitation (Kidd et al. 2017). Nowadays, satellite-based precipitation products are widely used as an alternative due to their higher spatial and temporal resolutions. Among satellite-based precipitation products, the Integrated Multi-satellite Retrievals for Global Precipitation Measurement (IMERG) data have fine spatial ( $\sim 0.1^\circ$ ) and temporal ( $\sim 30$  min) resolutions (Huffman et al. 2020). Tan et al. (2019) showed that the IMERG data adequately reproduce the diurnal variation of precipitation in Bangladesh. However, satellite-based precipitation products tend to show underestimation (overestimation) in the wet (dry) region and random errors due to the limitations in the precipitation retrieval algorithms and sampling frequency (Islam and Uyeda 2007; Nair et al. 2009). Therefore, it is necessary to evaluate satellite-based precipitation products with in situ observation before using them for precipitation analysis.

To investigate precipitation characteristics, the empirical orthogonal function (EOF) analysis method has been widely used. Using this method, Kripalani et al. (1996) analyzed monthly precipitation data from 1901 to 1977 in Bangladesh and found that the first and second EOF modes are associated with the inter-annual variation of monsoonal precipitation and the onset or withdrawal phase of monsoonal precipitation, respectively. The EOF analysis method, however, is known to have some limitations (Kim 2017). The EOF analysis method assumes that statistics (e.g., mean, variance, covariance) of variables are stationary, that is, do not change with time. In fact, however, statistics of many meteorological variables are non-stationary, changing with time. A non-stationary physical process changing with time cannot be represented by an individual EOF mode which is a single spatial pattern with a time-varying amplitude. The cyclostationary EOF (CSEOF) analysis method decomposes original data into multiple time-varying spatial patterns which are periodic in time, and each time-varying spatial pattern is regarded as a periodic physical process. This method assumes that statistics of variables are a periodic function

of time, which relaxes the assumption of the EOF analysis method. The CSEOF analysis method has been successfully used in analyses of climate data (Kullgren and Kim 2006; Kim et al. 2010; Roh et al. 2012; Kim and Kim 2020).

In this study, we evaluate the IMERG data against rain gauge observation to examine its usability in studies of precipitation in Bangladesh and surrounding regions. Then, we analyze the IMERG data using the CSEOF analysis method, focusing on the diurnal variation of precipitation in Bangladesh and surrounding regions. Section 2 describes the IMERG data and CSEOF analysis method. Section 3 presents the results and discussion. In Sect. 4, a summary is given.

## 2 IMERG data description and CSEOF analysis method

### 2.1 IMERG data description

As a next-generation satellite precipitation observation system, the Global Precipitation Measurement (GPM) mission was launched in February 2014 as a successor of TRMM (Hou et al. 2014; Yong et al. 2015). Accordingly, a new precipitation product made by GPM satellites, IMERG, became available to the public since January 2015, in place of an old precipitation product, TRMM Multi-satellite Precipitation Analysis (TMPA). The GPM satellites are equipped with upgraded instruments compared to the TRMM satellite. The use of a broader spectrum enables the GPM satellites to detect light precipitation better than the TRMM satellite. IMERG version 06B with a spatial resolution of  $0.1^\circ \times 0.1^\circ$  and a temporal resolution of 30 min is used in this study. For more detailed information about the IMERG data and the GPM mission, see Huffman et al. (2019, 2020).

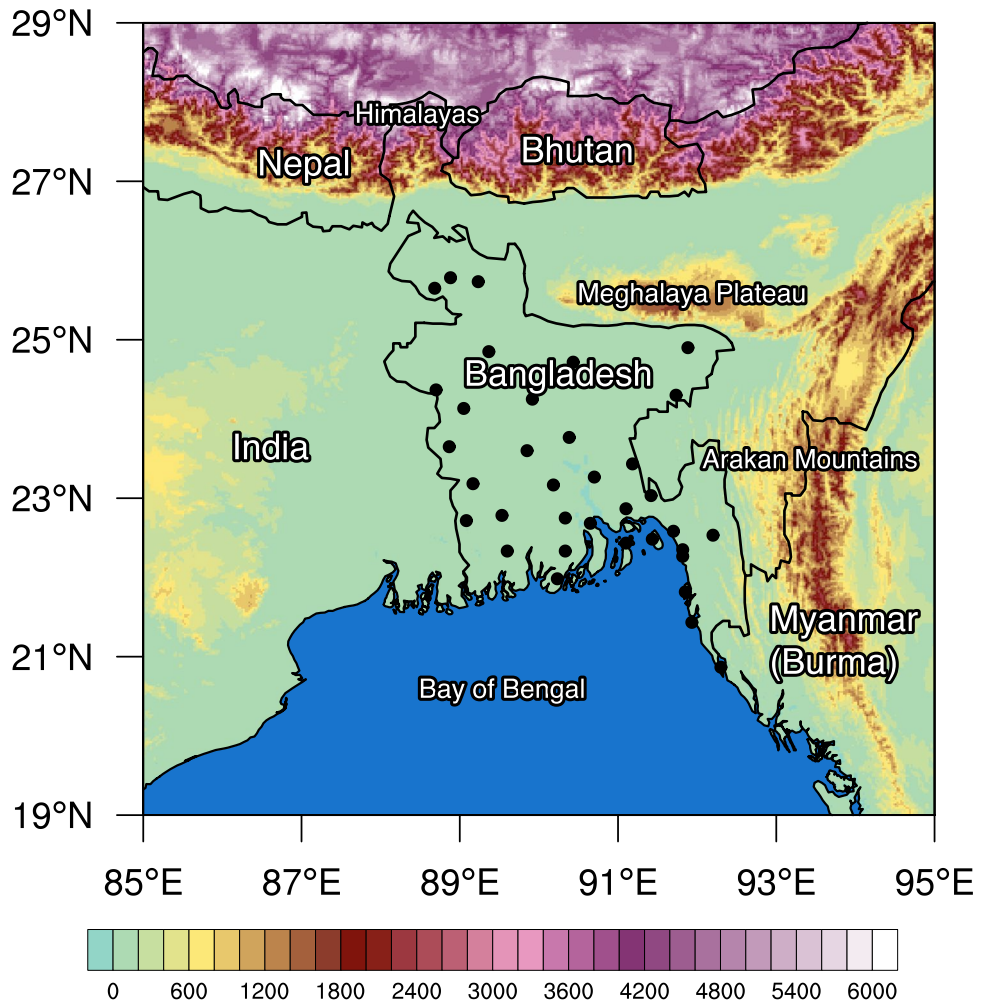
In this study, the 3-hourly rain gauge data from the Bangladesh Meteorological Department (BMD) during 2015–2019 are used for the evaluation of the IMERG data. Total 35 meteorological stations (Fig. 1) are spread in the country, but the data from Jessore ( $23.18^\circ\text{N}$ ,  $89.16^\circ\text{E}$ ) and Hatiya ( $22.43^\circ\text{N}$ ,  $91.10^\circ\text{E}$ ) are excluded from the analysis because of missing values.

### 2.2 CSEOF analysis method

In the CSEOF analysis method (Kim and North 1997; Kim et al. 2015; Kim 2017), original data  $T(r, t)$  called the target variable are decomposed as follows:

$$T(r, t) = \sum_n B_n(r, t) T_n(t). \quad (1)$$

**Fig. 1** Topographic map of Bangladesh and surrounding regions with the locations of 35 rain gauge stations (black circles)



Here,  $B_n(r, t)$  are decomposed spatio-temporal patterns called the CSEOF loading vectors (hereafter, CSLVs) and  $T_n(t)$  are corresponding time-varying amplitudes called the principal component time series (hereafter, PC time series).  $B_n(r, t)$  are periodic in time:

$$B_n(r, t) = B_n(r, t + d), \quad (2)$$

where  $d$  is the nested period. Each CSLV and its PC time series are collectively called a mode. Each mode is regarded as representing a distinct physical process.

In this study, the IMERG data are processed before the CSEOF analysis is conducted. First, the half-hourly IMERG data are converted to 3-hourly data for comparison with rain gauge data. Then, the 3-hourly data are averaged across the 5 years; for example, the precipitation amount during 0000–0300 LST on 1 January is obtained by averaging the precipitation amounts in the same time and date in the five different years. The CSEOF analysis is conducted for the pre-monsoon (March to May) and monsoon (June to September) seasons separately to find

characteristic precipitation patterns for each season. The nested period is set to 24 h to examine diurnal variations of precipitation in the pre-monsoon and monsoon seasons.

The main variable in this study is the anomaly of precipitation amount, computed by subtracting the seasonal-mean precipitation amount field. This variable is the target variable which is  $T(r, t)$  in Eq. (1). For each CSEOF mode of the target variable, spatio-temporal patterns of another variable (predictor variable,  $P(r, t)$ ), which are physically consistent with those of the target variable, can be obtained using the regression analysis in CSEOF space (Kim et al. 2015). Here, physical consistency means that two spatio-temporal patterns originated from different variables have identical time-varying amplitudes:

$$\{T(r,t), P(r,t)\} = \sum_n \{B_n(r,t), C_n^{(\text{reg})}(r,t)\} T_n(t), \quad (3)$$

where  $C_n^{(\text{reg})}(r, t)$  are the regressed spatio-temporal patterns extracted from the predictor variable. By conducting the regression analysis on other variables which are related

to the target variable, a mechanism corresponding to each CSEOF mode of the target variable can be suggested.

In this study, the reanalysis data from the European Centre for Medium-Range Weather Forecasts Reanalysis version 5 (ERA5, Hersbach et al. 2020) are used for the regression analysis. The anomaly of water vapor flux at 900 hPa is selected as a predictor variable and calculated from the wind vector and specific humidity in the hourly ERA5 data. The data of the predictor variable are processed using the same method used to process the IMERG data (i.e., converting to 3-hourly data, averaging across the 5 years). Note that when converting the hourly data to 3-hourly data, for example, generating the data during 0000–0300 LST (UTC + 6 h), the 3-hourly data at 0000, 0100, and 0200 LST are averaged. More detailed descriptions of the CSEOF analysis method and the regression analysis method are provided in Kim and North (1997), Kim et al. (2015), and Kim (2017).

### 3 Results and discussion

#### 3.1 Evaluation of IMERG data

In this subsection, the IMERG data in the period 2015–2019 are evaluated through the comparison with the rain gauge data provided by BMD. For the comparison, the IMERG data with  $0.1^\circ \times 0.1^\circ$  spatial resolution and 30-min time interval are bilinearly interpolated to the locations of the rain gauge stations and converted to 3-hourly data. The 3-h accumulated precipitation amounts from the IMERG data are compared with the rain gauge data in density scatter plots, for each season (Fig. 2). The density scatter plots show somewhat dispersed patterns of relative frequency. Overestimation of precipitation by the IMERG data occurs relatively frequently for very small precipitation amounts, and underestimation occurs relatively frequently for large precipitation amounts. The correlation coefficients between 3-hourly precipitation amounts from the IMERG data and those from the rain gauge data are 0.58, 0.58, and 0.60 for the pre-monsoon, monsoon, and post-monsoon seasons. The winter season when the seasonal precipitation amount is small shows a relatively low correlation coefficient (0.51). The IMERG data are known to have a better accuracy for a coarser temporal resolution, for example, for 1-day precipitation amounts (e.g., Tang et al. 2016). The correlation coefficients for 1-day precipitation amounts are 0.71, 0.76, 0.80, and 0.63 for the pre-monsoon, monsoon, post-monsoon, and winter seasons, which are much higher than those for 3-hourly precipitation amounts. This implies that the IMERG data can be used with a higher reliability for precipitation studies considering a larger time scale.

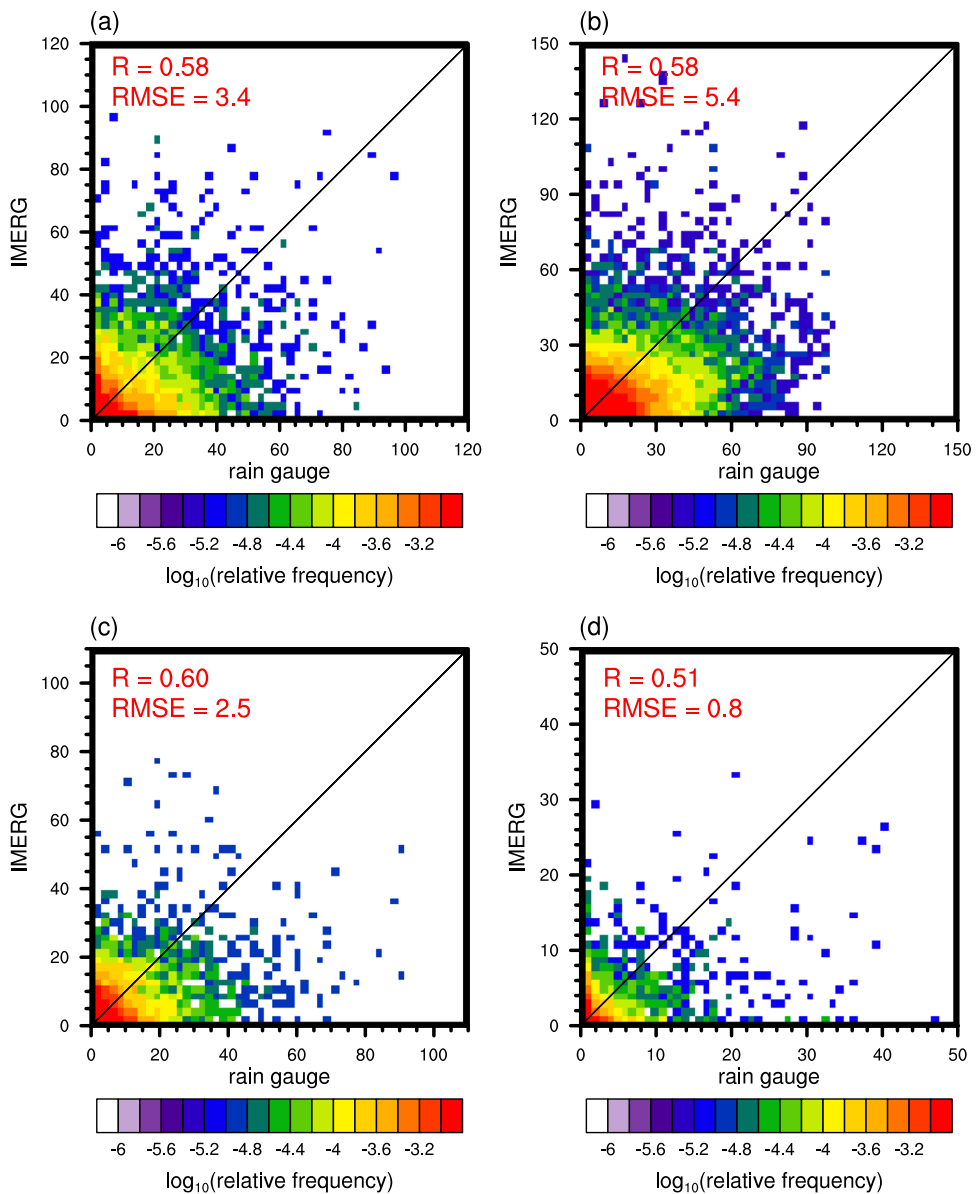
Latest versions of the IMERG data also provide the precipitation estimates for the period before the operation of the

GPM Core Observatory satellite, when the TRMM satellite was operating, using the data from the TRMM satellite. The IMERG data in this period (2003–2013) are less accurate than the data in the later period, showing lower correlation coefficients against the rain gauge data (0.54, 0.55, 0.57, and 0.44 for the pre-monsoon, monsoon, post-monsoon, and winter seasons). For this reason, only the IMERG data in the period 2015–2019 when the GPM Core Observatory satellite was operating are used for the evaluation in this study.

The comparison of precipitation amount in each season obtained from the rain gauge and IMERG data in Bangladesh is shown in Fig. 3. In the pre-monsoon season, the monthly mean precipitation amounts in the IMERG and rain gauge are 160 mm and 155 mm respectively, indicating a small overestimation (3%) in the IMERG. The IMERG well estimates the monthly mean precipitation amount in the monsoon season with a 6% overestimation. A relatively large overestimation (11%) is shown in the post-monsoon season. In the winter season, a negligible amount of precipitation is observed and the precipitation amount is overestimated in the IMERG. Overall, the IMERG estimates are in good agreement with the rain gauge observation.

The diurnal variation of precipitation is one of the most important features of precipitation in Bangladesh (Islam et al. 2005; Ahmed et al. 2020). Figure 4 shows the diurnal variations of precipitation amount in the country in each season revealed by both the IMERG and rain gauge data. The rain gauge shows that in the pre-monsoon season (Fig. 4a), the degree of diurnal variability is low and the precipitation maximum occurs during 0600–0900 LST. In contrast, the IMERG shows a higher degree of diurnal variability and the precipitation maximum occurs during 2100–0000 LST. The IMERG tends to underestimate precipitation during 0300–1200 LST, while it overestimates precipitation during 1200–0300 LST. In the monsoon season (Fig. 4b), precipitation exhibits a primary peak in the early morning (0300–0600 LST) and a secondary peak in the afternoon (1200–1500 LST) in both the IMERG and rain gauge. The IMERG identifies the two peaks in the rain gauge, with a slight underestimation (5%) for the primary peak and a slight overestimation (2%) for the secondary peak. It is also shown that the IMERG overestimates precipitation during 0900–0300 LST and underestimates precipitation during 0300–0900 LST. The diurnal variation of precipitation in the post-monsoon season (Fig. 4c) is quite different from that in the monsoon season. In the post-monsoon season, precipitation is decreased and its peak is shifted to a later time compared to the monsoon season, indicating a seasonal change of the diurnal variation of precipitation. The rain gauge shows a primary peak during 1200–1500 LST. The IMERG successfully captures the diurnal variation of precipitation pattern with a precipitation peak during 1200–1500 LST and a precipitation amount of 0.58 mm during 1200–1500

**Fig. 2** Density scatter plot between 3-hourly precipitation amounts (mm) from the IMERG data and those from the rain gauge data in the **a** pre-monsoon, **b** monsoon, **c** post-monsoon, and **d** winter seasons



LST that is the same as the rain gauge observation. However, precipitation is overestimated in other times. In the winter season (Fig. 4d), the diurnal variation of precipitation is somewhat similar to that in the monsoon season with a peak during 0300–0600 LST. The IMERG underestimates precipitation in times with relatively large precipitation amount (0300–0900 LST) and overestimates precipitation in times with relatively small precipitation amount (0900–2400 LST), showing a lower degree of diurnal variability than the rain gauge.

The spatial distributions of monthly mean precipitation amounts in the IMERG data are evaluated in Fig. 5. The observed spatial patterns of precipitation are overall well reproduced by the IMERG, while substantial overestimations and underestimations are found in some regions in some

seasons. In the pre-monsoon season, the underestimation of the monthly mean precipitation amount at Sylhet ( $24.90^{\circ}\text{N}$ ,  $91.88^{\circ}\text{E}$ ), located near the southern slope of the Meghalaya Plateau, is noticeable. In the monsoon season, the IMERG tends to overestimate precipitation in the western half of Bangladesh where the precipitation amounts are relatively small and it underestimates precipitation at Sylhet and some stations in the southeastern region where the precipitation amounts are relatively large. The largest overestimation in the monsoon season is found at Srimangal ( $24.30^{\circ}\text{N}$ ,  $91.73^{\circ}\text{E}$ ), located a little south of Sylhet where a significant underestimation occurs. The IMERG does not capture the drastic horizontal change in precipitation amount observed in the northeastern region of Bangladesh. Using the IMERG to investigate the local precipitation characteristics within

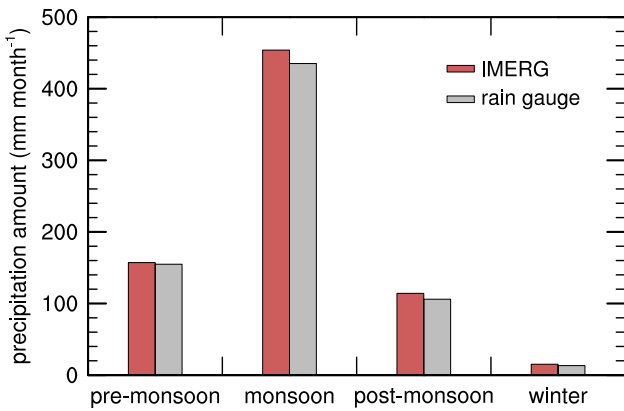


**Fig. 3** Seasonal variations of monthly mean precipitation amount averaged over the period 2015–2019 for the IMERG data and rain gauge data

the northeastern region of Bangladesh should be done with extra care. In the post-monsoon season, overestimations are found at a majority of rain gauge stations. In the winter season, big relative differences are found at some stations in the

northwestern and southeastern regions where the observed precipitation amounts are very small and overestimated by the IMERG.

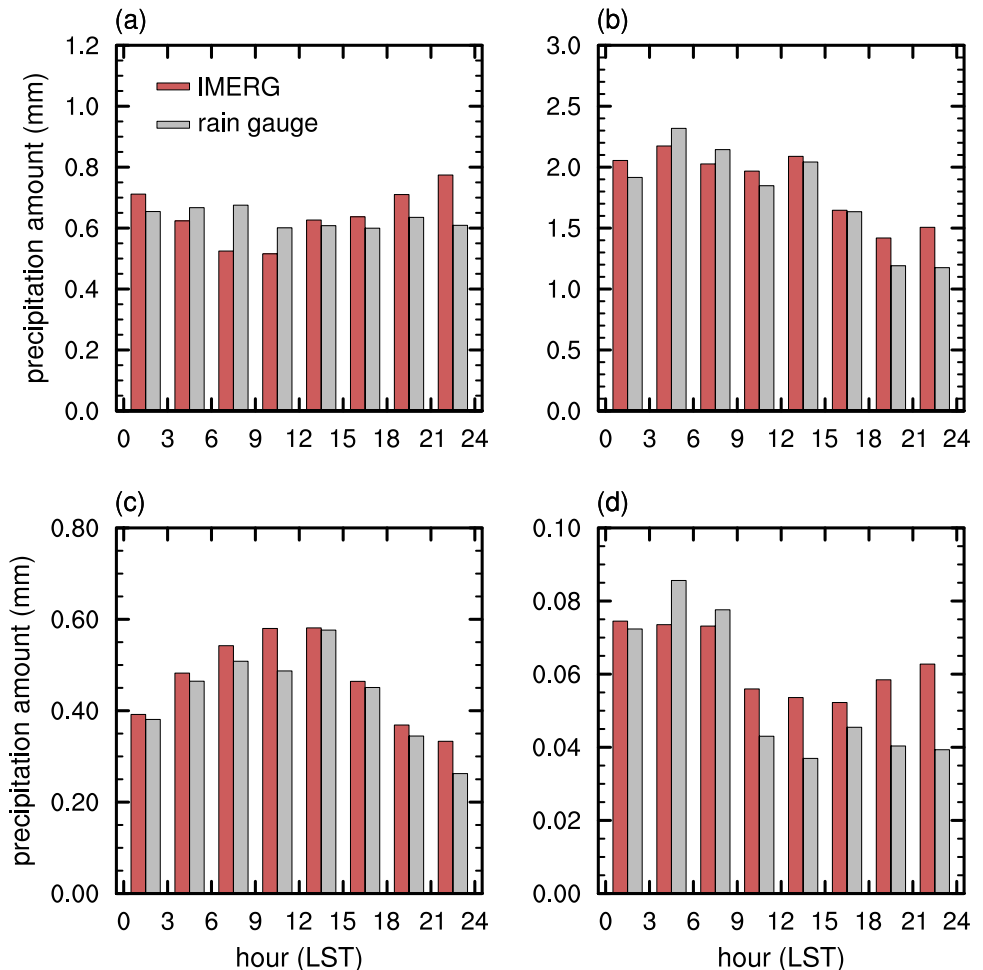
The IMERG well reproduces the seasonal variation of precipitation. For the diurnal variation of precipitation, the IMERG captures the overall patterns despite some overestimations and underestimations. The spatial distribution of precipitation is also captured well, except for the northeastern region which exhibits the drastic horizontal change in precipitation amount. These results suggest that the IMERG precipitation product can be used for studying the spatio-temporal variations of precipitation in Bangladesh, with a proper consideration of the revealed biases.

### 3.2 CSEOF analysis

#### 3.2.1 Pre-monsoon

Figure 6 shows the fields of diurnal variations of the first and second CSLVs of precipitation amount anomaly in the pre-monsoon season, and Fig. 7 shows the corresponding PC time series. The first CSLV is characterized by strong

**Fig. 4** Diurnal variations of 3-hourly precipitation amount in the **a** pre-monsoon, **b** monsoon, **c** post-monsoon, and **d** winter seasons averaged over the period 2015–2019 for the IMERG data and rain gauge data



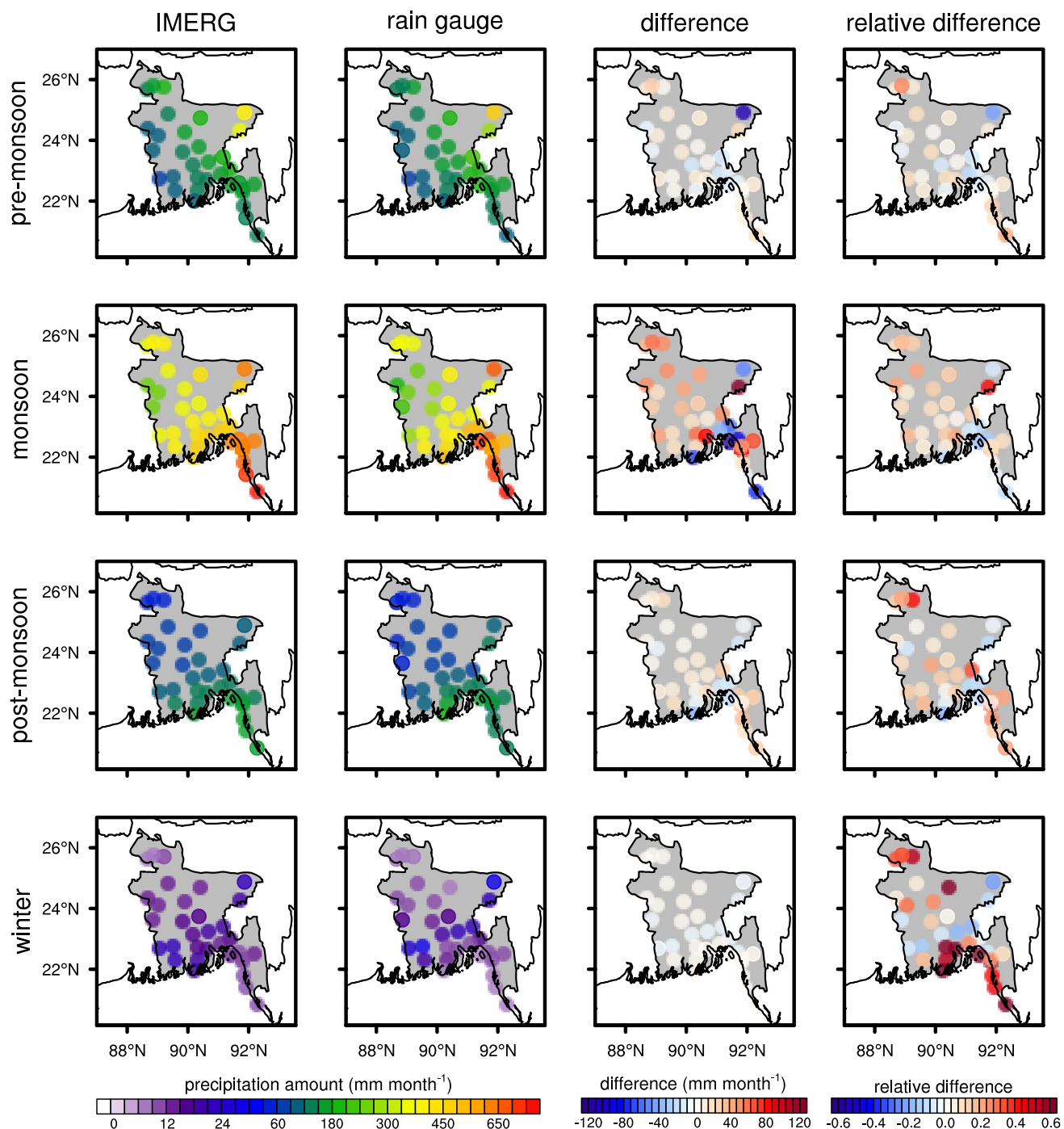


**Fig. 5** Spatial distributions of monthly mean precipitation amounts in the pre-monsoon (first row), monsoon (second row), post-monsoon (third row), and winter (fourth row) seasons averaged over the period

2015–2019 for the IMERG data (first column), rain gauge data (second column), their differences (IMERG—rain gauge) (third column), and their relative differences (fourth column)

positive precipitation anomalies in the northern region of Bangladesh and the Meghalaya Plateau region during 0000–0600 LST. These anomalies are weakened in the daytime and strengthened in the late night, exhibiting a clear diurnal cycle. During 1800–2100 LST, the central region of the country exhibits a relatively strong positive anomaly

compared to other regions. The PC time series of the first CSEOF mode shows that the amplitude of the diurnal cycle is relatively small in March, and it grows overall from mid-April to late May. The peak times of precipitation anomalies in the northern and central regions of Bangladesh are consistent with the peak times of pre-monsoonal precipitation

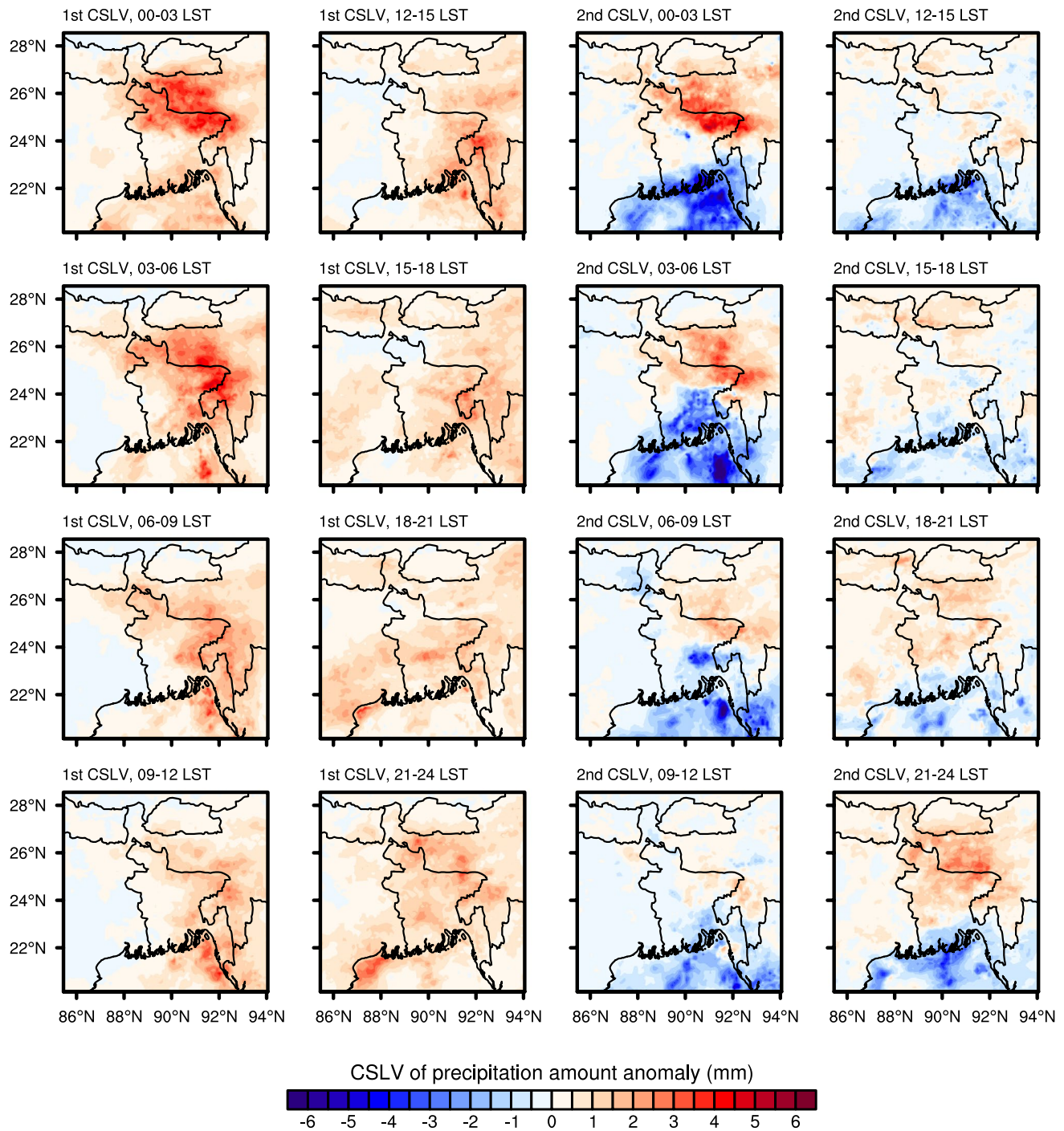


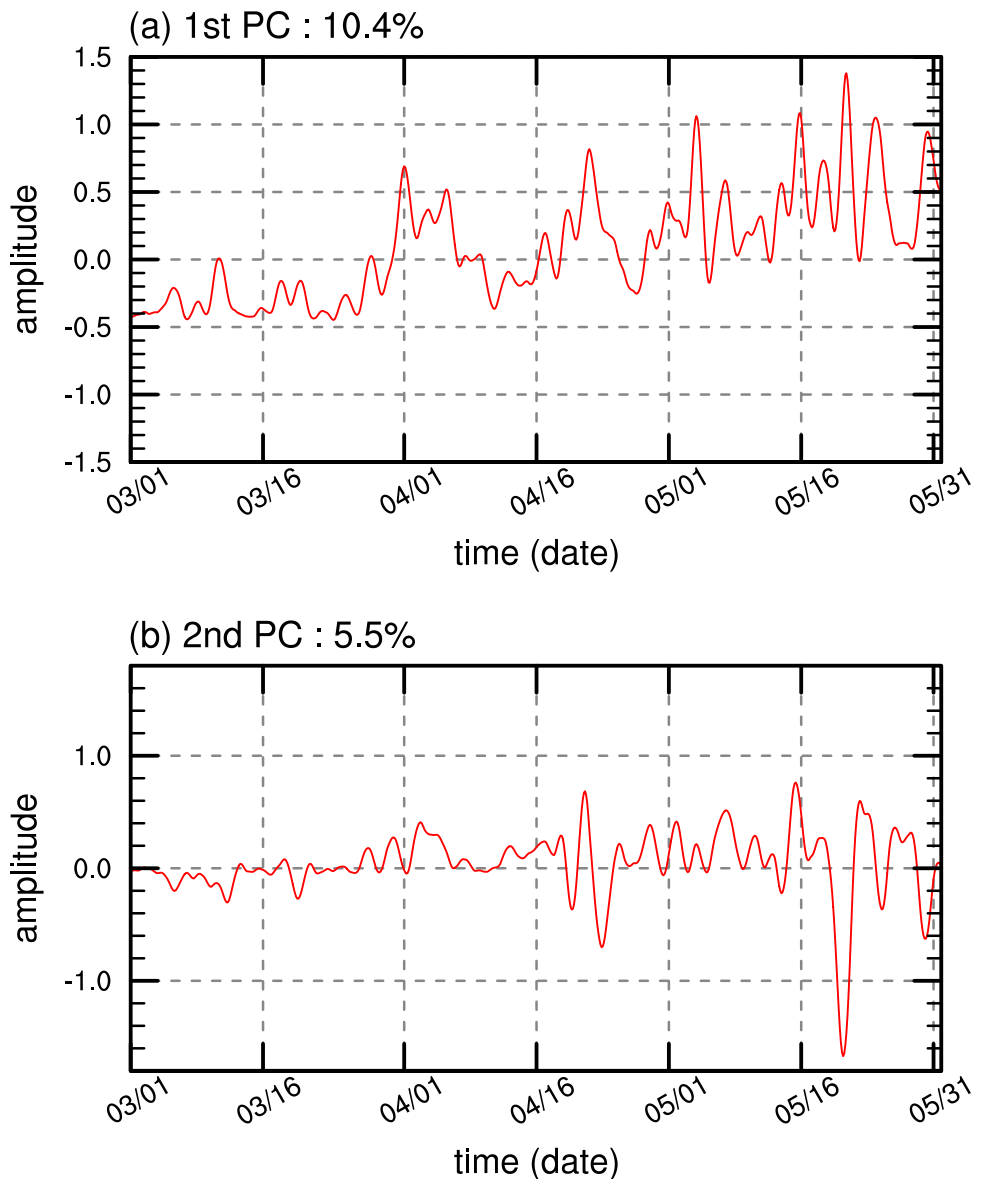
**Fig. 6** 3-hourly CSLVs for the first (two leftmost columns) and second (two rightmost columns) CSEOF modes of precipitation amount anomaly in the pre-monsoon season

in those regions, implying that the first mode represents the general characteristics of the diurnal variation of precipitation. The first mode contributes 10.4% to the total variance of the pre-monsoonal precipitation.

The second CSLV is characterized by strong positive precipitation anomalies in the northeastern region of

Bangladesh and the Meghalaya Plateau region and strong negative precipitation anomalies in the southern region of the country and the northern region of the Bay of Bengal (BOB) during 0000–0600 LST. The PC time series of the second CSEOF mode is mostly in a positive phase since late March. The positive phase indicates the enhancement

**Fig. 7** PC time series for the **a** first and **b** second CSEOF modes of precipitation amount anomaly in the pre-monsoon season



of precipitation in the northern region of Bangladesh and the Meghalaya Plateau region and the suppression of precipitation in the southern region of Bangladesh and the northern region of the BOB. The second mode that represents the north–south precipitation difference contributes 5.5% to the total variance of the pre-monsoonal precipitation.

Figure 8 shows the fields of diurnal variations of CSLVs of 900-hPa water vapor flux anomaly regressed to the first and second modes of the pre-monsoonal precipitation anomaly. In the first regressed mode, the water vapor flux anomaly is southwesterly over the BOB and mainly southerly in Bangladesh, indicating the enhancement of moisture transport from the BOB to inland Bangladesh. The southern slope of the Meghalaya Plateau exhibits southerly water vapor flux anomaly during 0000–0600 LST and southeasterly water vapor flux anomaly during 0900–1500 LST. Because

the southern slope of the Meghalaya Plateau is east–west oriented, the enhancement of the meridional component of water vapor flux anomaly in this region during 0000–0600 LST results in stronger orographic lifting and upward moisture transport. This can intensify precipitation in the plateau and surrounding regions in this time, which is represented by the strong positive precipitation anomalies (Fig. 6). The strengthening of the diurnal cycle of precipitation since mid-April is linked with the enhancement of the water vapor flux anomaly in the same period (Fig. 7a).

In the second regressed mode, the water vapor flux anomaly in Bangladesh is relatively strong, while it is relatively weak in the northern region of the BOB. In contrast with the first regressed mode, the second regressed mode shows the spatial pattern of water vapor flux anomaly that varies substantially with time. During 0000–0900 LST, the water

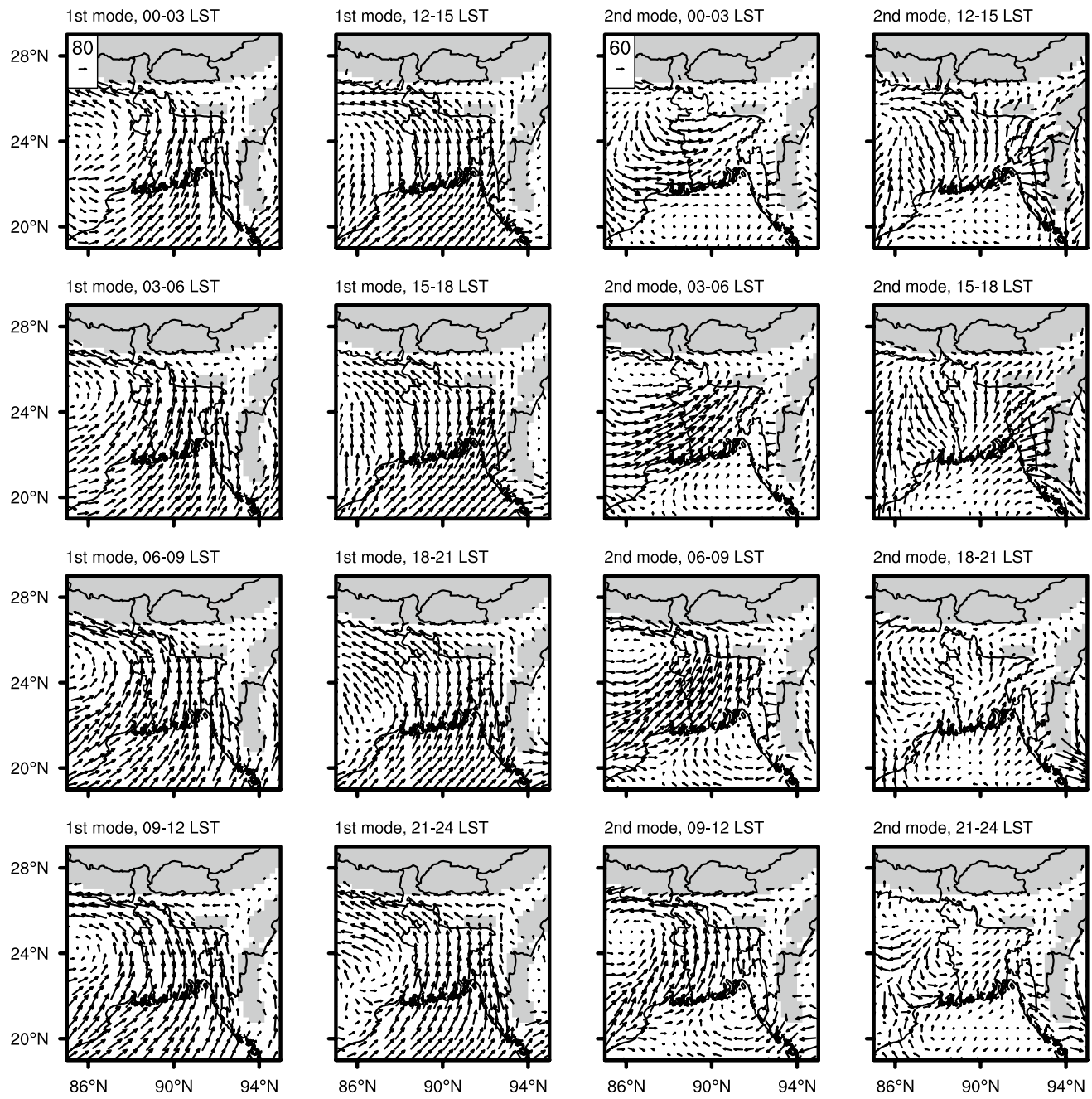


**Fig. 8** Regressed 3-hourly CSLVs of 900-hPa water vapor flux anomaly ( $\text{g kg}^{-1} \text{m s}^{-1}$ ) associated with the first (two leftmost columns) and second (two rightmost columns) CSEOF modes of precipitation amount anomaly in the pre-monsoon season

vapor flux anomaly is mostly directed toward the BOB at the east coast of India and the west coast of Myanmar. In contrast, during 1500–2100 LST, the water vapor flux anomaly is mostly directed toward land at the coasts. These can be somewhat attributed to the land-sea breeze circulation in the coastal regions along with the mountain-valley breeze circulation around the Arakan Mountains. The southwesterly water vapor flux anomaly in Bangladesh is strong during 0000–0900 LST, indicating that the precipitation anomalies

in the northeastern region and the Meghalaya Plateau region in this time in this mode are associated with the enhancement of southwesterly moisture transport, which does not directly come from the BOB. On the other hand, the suppression of precipitation in the northern region of the BOB in this mode can be linked with the relatively weak water vapor flux anomaly in this region. When the PC time series is in a negative phase, the southwesterly water vapor flux anomaly in Bangladesh during 0000–0900 LST is reversed and it

acts against the mean southwesterly water vapor flux in the pre-monsoon season. The weakening of moisture transport approaching the southern slope of the Meghalaya Plateau reduces the precipitation in the northeastern region of Bangladesh and the Meghalaya Plateau region and enhances the precipitation in the southern region of Bangladesh and the northern region of the BOB.

### 3.2.2 Monsoon

The fields of diurnal variations of the first and second CSLVs of precipitation amount anomaly in the monsoon season and corresponding PC time series are presented in Figs. 9 and 10, respectively. The first CSLV is characterized by strong positive precipitation anomalies in the northern region of the BOB during 0600–1500 LST and in the southeastern region of Bangladesh during 1200–1500 LST. The precipitation anomaly in the northern region of the BOB starts to develop during 0000–0300 LST, peaks during 0600–0900 LST, and is weakened during 1200–1500 LST, exhibiting a clear diurnal cycle. The PC time series of the first CSEOF mode has small values in most of the time, but its values soar at some specific times. This means that this mode is strongly activated occasionally but deactivated ordinarily. The first mode contributes 14.4% to the total variance of the monsoonal precipitation.

The second CSLV is characterized by strong positive precipitation anomalies in the northeastern region of Bangladesh and the southern slopes of the Meghalaya Plateau and Himalayan Foothills during 0000–0600 LST and in the northwestern region of the BOB during 0600–1200 LST. In the southwestern region of Bangladesh, the precipitation anomaly peaks during 1200–1500 LST. The precipitation anomaly peaks in the Arakan Mountains during 1500–1800 LST. The PC time series of the second CSEOF mode is in a positive phase in most of the time in the monsoon season. The peak times of precipitation anomalies in the northern and southwestern regions of Bangladesh roughly match with the peak times of monsoonal precipitation in these regions (Ahmed et al. 2020). During 1500–1800 LST, the precipitation anomalies in the southeastern coastal region of Bangladesh and the nearby region close to the Arakan Mountains show a big contrast. This difference is confirmed by both the IMERG and rain gauge data (not shown). The high spatial resolution of the IMERG data can play an important role in identifying such a big contrast in the region where rain gauge stations are sparsely distributed. The second mode contributes 5.6% to the total variance of the monsoonal precipitation.

The fields of diurnal variations of CSLVs of 900-hPa water vapor flux anomaly regressed to the first and second modes of the monsoonal precipitation anomaly are presented in Fig. 11. Note that the mean 900-hPa water vapor flux in

the monsoon season is southwesterly in the northern region of the BOB and mainly southerly in Bangladesh (Ahmed et al. 2020). In the first regressed mode, a strong westerly water vapor flux anomaly prevails in the northern region of the BOB and it is deflected northward by the Arakan Mountains. The spatial patterns of water vapor flux anomaly in this mode do not show a strong diurnal variation. The magnitude of water vapor flux anomaly in the northern region of the BOB is largest during 0900–1200 LST, and the convergence of water vapor flux anomaly in the southeastern region of Bangladesh is largest during 1200–1500 LST (not shown). This indicates that if a strong westerly anomaly prevails in the northern region of the BOB, the moist wind climbs the slope of the Arakan Mountains, piling moisture in the southeastern region of Bangladesh and resulting in maximum precipitation anomaly there during 1200–1500 LST. The peak time of precipitation anomaly in the northern region of the BOB agrees with that of the magnitude of 900-hPa water vapor flux in the northern region of the BOB. This characteristic moisture transport pattern occasionally occurs in the monsoon season (Fig. 10a), enhancing precipitation in the northern region of the BOB and the southeastern region of Bangladesh.

The second regressed mode shows a relatively strong diurnal variation of the spatial patterns of water vapor flux anomaly. A strong southwesterly water vapor flux anomaly is directed toward the southern slopes of the Meghalaya Plateau and Himalayan Foothills during 0000–0600 LST. Taking into account that the mean water vapor flux in the monsoon season is southerly, the strong southwesterly water vapor flux anomaly in the nighttime makes a large amount of moisture directly reach the southern slopes of the Meghalaya Plateau and Himalayan Foothills without facing any other orographic obstacles (e.g., the Arakan Mountains), which results in the strong positive precipitation anomalies in these regions during 0000–0600 LST in this mode. After ~0600 LST, a cyclonic circulation anomaly centered in the northwestern region of the BOB develops and it weakens the water vapor flux heading toward the southern slopes of the Meghalaya Plateau and Himalayan Foothills, which can be associated with the weakened precipitation anomalies in these regions in this time, as shown in Fig. 9. An ascending motion produced by this cyclonic circulation anomaly could be suggested as a driving mechanism for the strong positive precipitation anomaly in the northwestern region of the BOB during 0600–1200 LST. From ~1500 LST, the cyclonic circulation anomaly disappears, making precipitation in the northwestern region of the BOB reduced.

Fujinami et al. (2017) reported that precipitation around the Meghalaya Plateau in the monsoon season can be classified into easterly and westerly regimes of the intra-seasonal oscillation, determined by the low-level wind direction in the windward region of the plateau. The

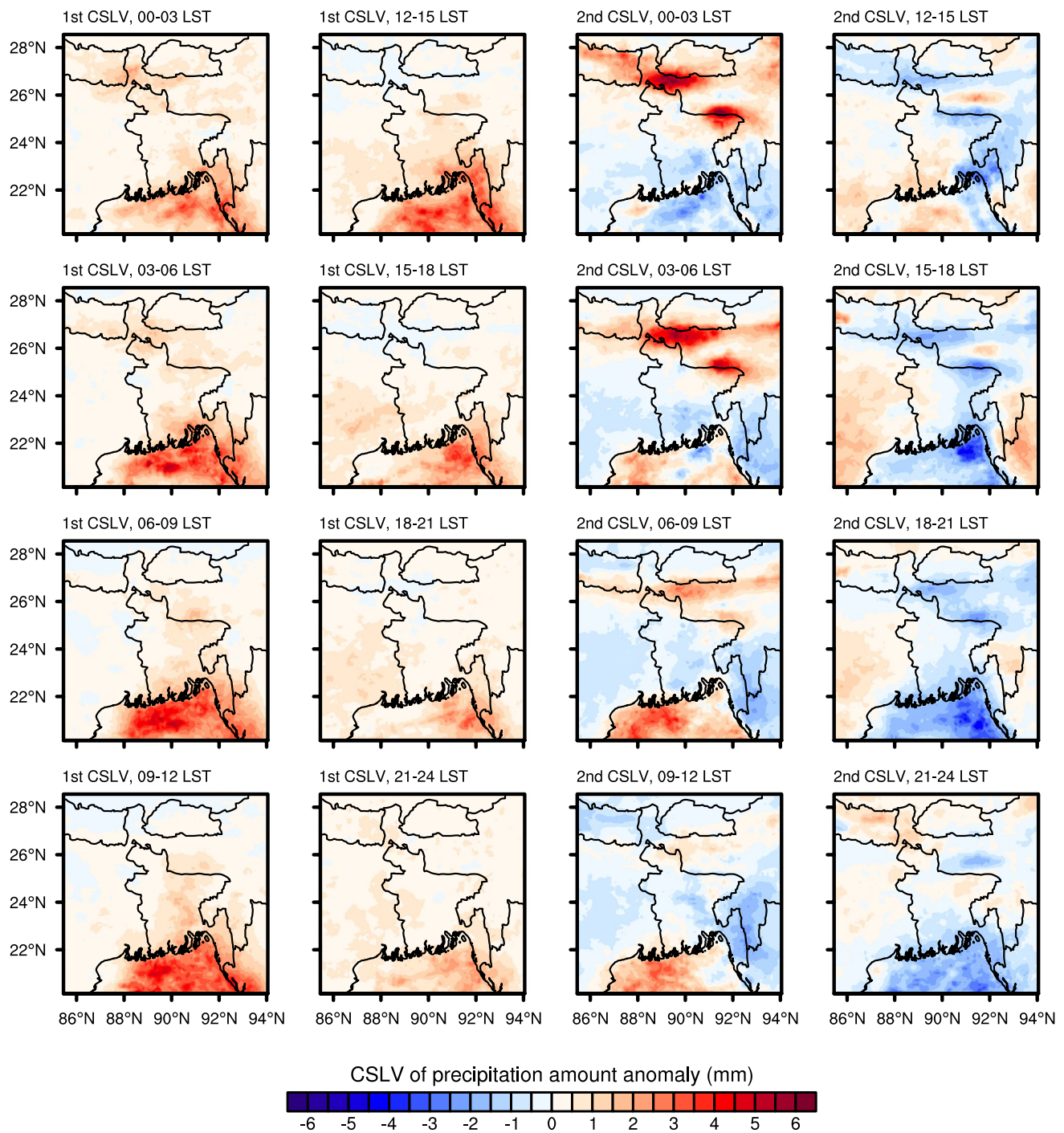
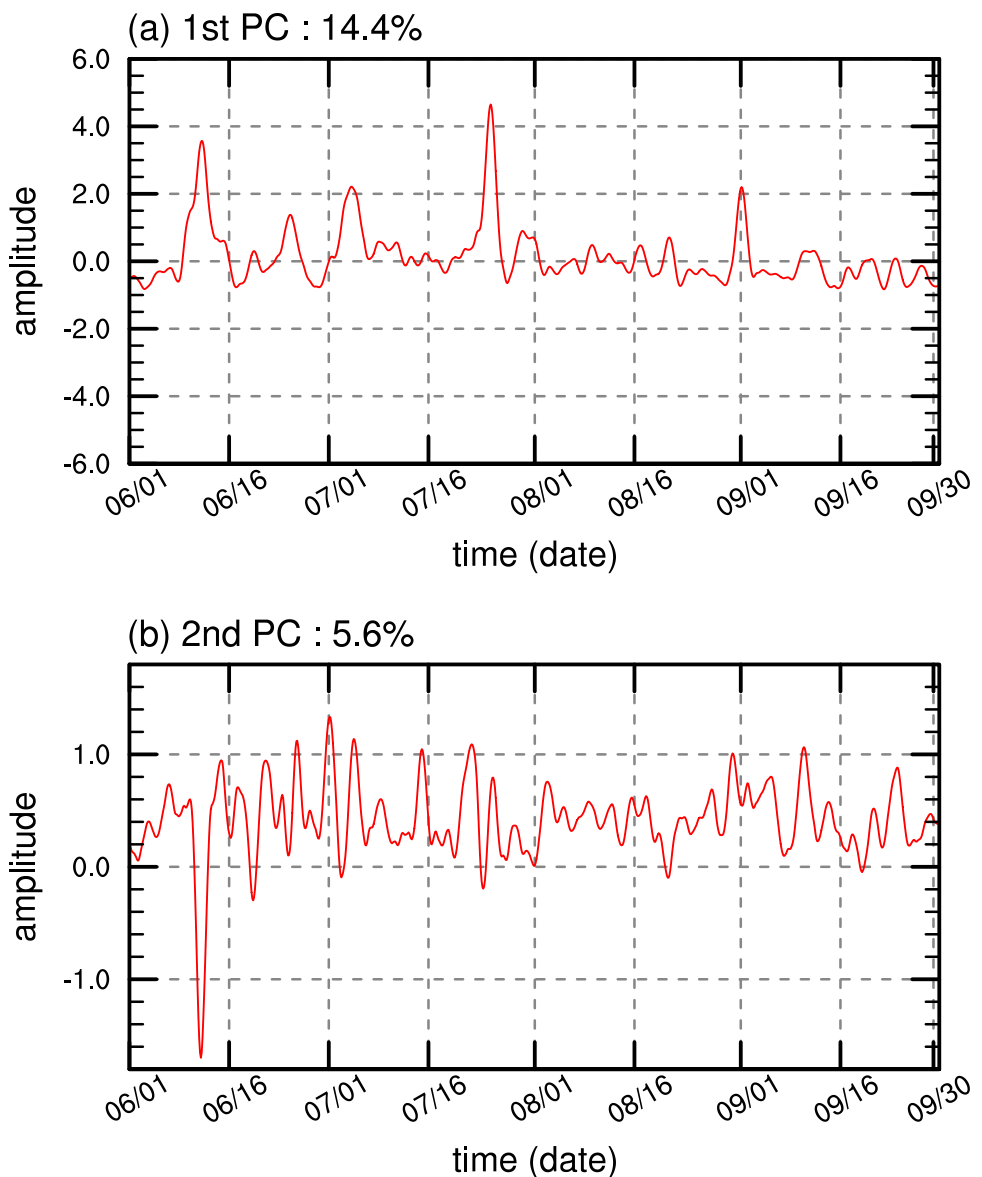


**Fig. 9** As in Fig. 6, but for the monsoon season

precipitation and wind patterns of the first and second modes in the monsoon season are very similar to those of the easterly and westerly regimes in Fujinami et al. (2017), respectively. The connection between the first two CSEOF modes and the two different regimes of the intra-seasonal oscillation deserves a further investigation.

The contributions of the first CSEOF modes to the total variance of pre-monsoonal and monsoonal precipitation (10.4% and 14.4%, respectively) in this study are small compared to those in some previous studies using monthly precipitation data (e.g., Sun et al. 2021). However, studies that used 5-day and daily precipitation data for the CSEOF

**Fig. 10** As in Fig. 7, but for the monsoon season



analysis (Kullgren and Kim 2006; Kim et al. 2010) also obtained the relatively small contribution of the first mode (~16%), which could be attributed to the higher complicatedness of the daily variation of precipitation compared to the monthly variation. The contributions of the first modes in those previous studies are comparable to those in this study.

#### 4 Summary

This study evaluates the applicability of a satellite retrieval-based precipitation dataset, IMERG, to research on precipitation in Bangladesh and surrounding regions. The IMERG data successfully reproduce the observed seasonal variation of precipitation. The diurnal variation of precipitation is also generally well reproduced by the

IMERG data, except for the overestimation of the degree of diurnal variability in the pre-monsoon season. Large underestimations of precipitation are found at Sylhet in the pre-monsoon and monsoon seasons, where the observed precipitation amounts are large and the IMERG data underestimate them.

Because the correlation between 3-hourly precipitation amounts in the IMERG data and those in the rain gauge data is not very high ( $R=0.51\text{--}0.60$ ) and underestimations of heavy precipitation and overestimations of light precipitation are frequent, the use of the IMERG data for studying short-term individual precipitation events in Bangladesh and surrounding regions should be done with extra care. On the other hand, the IMERG data well reproduce the observed patterns of spatial and temporal distributions of precipitation averaged over a relatively long period, which encourages the

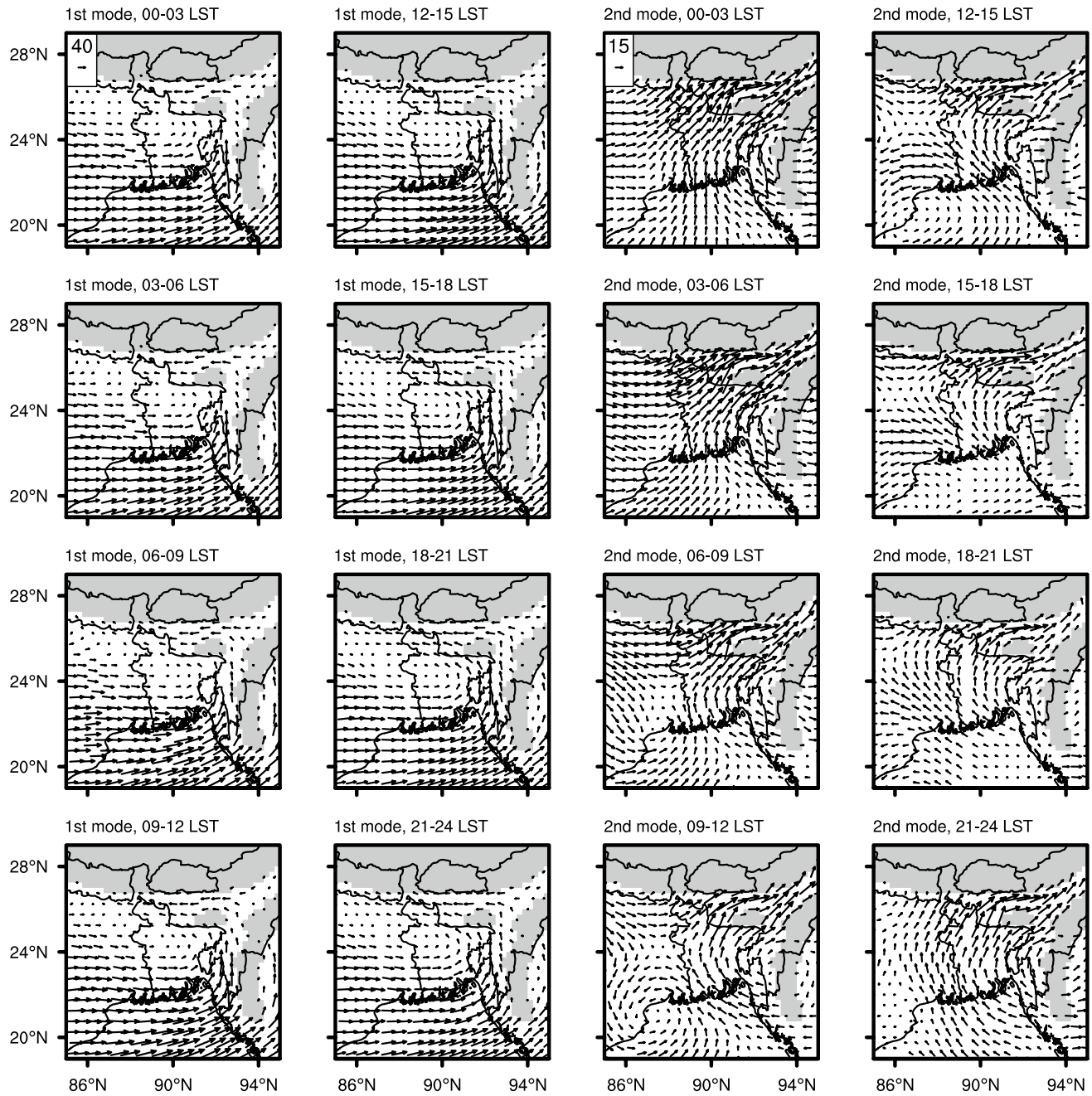


**Fig. 11** As in Fig. 8, but for the monsoon season

use of the IMERG data for studying general precipitation characteristics in this region.

The IMERG data are used in the CSEOF analysis to examine important features of the diurnal variations of pre-monsoonal and monsoonal precipitation in Bangladesh and surrounding regions and their relationship with the low-level water vapor flux. The first mode of pre-monsoonal precipitation is characterized by enhanced precipitation in the northern region of Bangladesh and the Meghalaya Plateau region in the late night to early morning, which

is related to the enhancement of the southerly component of moisture transport from the BOB to the southern slope of the Meghalaya Plateau. The second mode represents a north-south difference in precipitation which also becomes large in the late night to early morning, and this is linked with the diurnal variation of southwesterly moisture transport over Bangladesh.

For precipitation in the monsoon season, the first and second CSEOF modes show contrasting CSLV patterns. The first mode shows enhanced precipitation in the northern

region of the BOB during 0600–1500 LST, which is related to the strengthening of westerly moisture transport over the BOB toward the Arakan Mountains in this time. In contrast, the second mode shows enhanced precipitation in the southern slopes of the Meghalaya Plateau and Himalayan Foothills during 0000–0600 LST, which is related to the southwesterly moisture transport being neither blocked nor deflected by the Arakan Mountains.

**Acknowledgements** The authors thank the Bangladesh Meteorological Department for providing the rain gauge data.

**Author contributions** Jong-Jin Baik designed this study. Tanvir Ahmed and Seong-Ho Hong performed the data analysis and visualization. All authors discussed the results. Tanvir Ahmed, Seong-Ho Hong, and Han-Gyul Jin wrote the initial draft. Jong-Jin Baik, Han-Gyul Jin, and Joohyun Lee reviewed and corrected the manuscript. All authors read and approved the final version of the manuscript.

**Funding** This work was supported by the National Research Foundation of Korea (NRF) under grants 2019R1A6A1A10073437 and 2021R1A2C1007044.

**Availability of data and material** The IMERG data used in this study were provided by the NASA Goddard Earth Sciences Data and Information Services Center. The rain gauge data were provided by the Bangladesh Meteorological Department.

**Code availability** The codes used for analyses in this study can be obtained from the corresponding author if necessary.

## Declarations

**Ethics approval** Not applicable.

**Consent to participate** Not applicable.

**Consent for publication** Not applicable.

**Conflict of interest** The authors declare no competing interests.

## References

- Ahmed R, Kim I-K (2003) Patterns of daily rainfall in Bangladesh during the summer monsoon season: case studies at three stations. *Phys Geogr* 24:295–318
- Ahmed T, Jin H-G, Baik J-J (2020) Spatiotemporal variations of precipitation in Bangladesh revealed by nationwide rain gauge data. *Asia-Pac J Atmos Sci* 56:593–602
- Chowdhury AFMK, Kar KK, Shahid S, Chowdhury R, Rashid MM (2019) Evaluation of spatio-temporal rainfall variability and performance of a stochastic rainfall model in Bangladesh. *Int J Climatol* 39:4256–4273
- Fujinami H, Hatsuzuka D, Yasunari T, Hayashi T, Terao T, Murata F, Kiguchi M, Yamane Y, Matsumoto J, Islam MN, Habib A (2011) Characteristic intraseasonal oscillation of rainfall and its effect on interannual variability over Bangladesh during boreal summer. *Int J Climatol* 31:1192–1204
- Fujinami H, Sato T, Kanamori H, Murata F (2017) Contrasting features of monsoon precipitation around the Meghalaya Plateau under westerly and easterly regimes. *J Geophys Res: Atmos* 122:9591–9610
- He X, Vejen F, Stisen S, Sonnenborg TO, Jensen KH (2011) An operational weather radar-based quantitative precipitation estimation and its application in catchment water resources modeling. *Vadose Zone J* 10:8–24
- Hersbach H, Bell B, Berrisford P, Hirahara S, Horányi A, Muñoz-Sabater J, Nicolas J, Peubey C, Radu R, Schepers D, Simmons A, Soci C, Abdalla S, Abellan X, Balsamo G, Bechtold P, Biavati G, Bidlot J, Bonavita M, Chiara G, Dahlgren P, Dee D, Diamantakis M, Dragani R, Flemming J, Forbes R, Fuentes M, Geer A, Haimberger L, Healy S, Hogan RJ, Hólm E, Janisková M, Keeley S, Laloyaux P, Lopez P, Lupu C, Radnoti G, Rosnay P, Rozum I, Vamborg F, Villaume S, Thépaut J-N (2020) The ERA5 global reanalysis. *Q J R Meteorol Soc* 146:1999–2049
- Hou AY, Kakar RK, Neeck S, Azarbarzin AA, Kummerow CD, Kojima M, Oki R, Nakamura K, Iguchi T (2014) The Global Precipitation Measurement mission. *Bull Am Meteorol Soc* 95:701–722
- Huffman GJ, Bolvin DT, Braithwaite D, Hsu K, Joyce R, Kidd C, Nelkin EJ, Sorooshian S, Tan J, Xie P (2019) Algorithm Theoretical Basis Document (ATBD) Version 06. NASA Global Precipitation Measurement (GPM) Integrated Multi-Satellite Retrievals for GPM (IMERG). NASA. Available from <https://gpm.nasa.gov/>
- Huffman GJ, Bolvin DT, Nelkin EJ, Tan J (2020) Integrated Multi-satellite Retrievals for GPM (IMERG) technical documentation. NASA/GSFC. Available from <https://gpm.nasa.gov/>
- Islam MN, Uyeda H (2007) Use of TRMM in determining the climatic characteristics of rainfall over Bangladesh. *Remote Sens Environ* 108:264–276
- Islam MN, Terao T, Uyeda H, Hayashi T, Kikuchi K (2005) Spatial and temporal variations of precipitation in and around Bangladesh. *J Meteorol Soc Jpn* 83:21–39
- Kidd C, Becker A, Huffman GJ, Muller CL, Joe P, Skofronick-Jackson G, Kirschbaum DB (2017) So, how much of the Earth's surface is covered by rain gauges? *Bull Am Meteorol Soc* 98:69–78
- Kim K-Y (2017) Cyclostationary EOF analysis: theory and applications. Seoul National University Press, Seoul
- Kim K-Y, Kim B-S (2020) The effect of regional warming on the East Asian summer monsoon. *Clim Dyn* 54:3259–3277
- Kim K-Y, North GR (1997) EOFs of harmonizable cyclostationary processes. *J Atmos Sci* 54:2416–2427
- Kim K-Y, Roh J-W, Lee D-K, Jhun J-G (2010) Physical mechanisms of the seasonal, subseasonal, and high-frequency variability in the seasonal cycle of summer precipitation in Korea. *J Geophys Res* 115:D14110
- Kim K-Y, Hamlington B, Na H (2015) Theoretical foundation of cyclostationary EOF analysis for geophysical and climatic variables: concepts and examples. *Earth-Sci Rev* 150:201–218
- Kripalani RH, Inamdar S, Sontakke NA (1996) Rainfall variability over Bangladesh and Nepal: comparison and connections with features over India. *Int J Climatol* 16:689–703
- Kullgren K, Kim K-Y (2006) Physical mechanisms of the Australian summer monsoon: 1. seasonal cycle. *J Geophys Res* 111:D20104
- Mohsenipour M, Shahid S, Ziarh GF, Yaseen ZM (2020) Changes in monsoon rainfall distribution of Bangladesh using quantile regression model. *Theor Appl Climatol* 142:1329–1342
- Murata F, Terao T, Hayashi T, Asada H, Matsumoto J (2008) Relationship between atmospheric conditions at Dhaka, Bangladesh, and rainfall at Cherrapunjee, India. *Nat Hazards* 44:399–410
- Nair S, Srinivasan G, Nemani R (2009) Evaluation of multi-satellite TRMM derived rainfall estimates over a western state of India. *J Meteorol Soc Jpn* 87:927–939

- Roh J-W, Kim K-Y, Jhun J-G (2012) Decadal changes in the physical mechanisms of the seasonal cycle of summertime precipitation variability in Korea. *J Geophys Res* 117:D07115
- Shahid S, Khairulmaini OS (2009) Spatio-temporal variability of rainfall over Bangladesh during the time period 1969–2003. *Asia-Pac J Atmos Sci* 45:375–389
- Sun M, Kim G, Xu X, Wang Y (2021) Investigation of South Korea precipitation variation using empirical orthogonal function (EOF) and cyclostationary EOF. *IOF Conf Ser Earth and Environ Sci* 643:012084
- Tan J, Huffman GJ, Bolvin DT, Nelkin EJ (2019) Diurnal cycle ofIMERG V06 precipitation. *Geophys Res Lett* 46:13584–13592
- Tang G, Ma Y, Long D, Zhong L, Hong Y (2016) Evaluation of GPM Day-1 IMERG and TMPA Version-7 legacy products over Mainland China at multiple spatiotemporal scales. *J Hydrol* 533:152–167
- Tarek MH, Hassan A, Bhattacharjee J, Choudhury SH, Badruzzaman ABM (2017) Assessment of TRMM data for precipitation measurement in Bangladesh. *Meteorol Appl* 24:349–359
- Yong B, Liu D, Gourley JJ, Tian Y, Huffman GJ, Ren L, Hong Y (2015) Global view of real-time TRMM multisatellite precipitation analysis: implications for its successor Global Precipitation Measurement mission. *Bull Am Meteorol Soc* 96:283–296

**Publisher's note** Springer Nature remains neutral with regard to jurisdictional claims in published maps and institutional affiliations.